Nature Communications

https://doi.org/10.1038/s41467-025-66882-7

Article in Press

Optimizing thiamine pyrophosphate metabolism enhances crop yield and quality

Received: 22 March 2025

Accepted: 18 November 2025

Cite this article as: Luo, Y., Liu, Y., Liu, J. *et al.* Optimizing thiamine pyrophosphate metabolism enhances crop yield and quality. *Nat Commun* (2025). https://doi.org/10.1038/s41467-025-66882-7

Yun Luo, Yu Liu, Jie Liu, Xiaojing Liu, Huinan Li, Yu Wu, Junli Zhao, Yuebin Wang, Wenjie Fang, Liumei Jian, Lin Zhuo, Wenqiang Li, Junpeng Zhan, Alisdair R. Fernie & Jianbing Yan

Optimizing thiamine pyrophosphate metabolism enhances crop yield and quality

Yun Luo[1, 2 §], Yu Liu[1, 2 §], Jie Liu[3], Xiaojing Liu[1, 2], Huinan Li[1, 2], Yu Wu[4], Junli Zhao[4], Yuebin Wang[1, 2], Wenjie Fang[1, 2], Liumei Jian[1, 2], Lin Zhuo[1, 2], Wenqiang Li[1, 2], Junpeng Zhan[1, 2], Alisdair R. Fernie[5], Jianbing Yan[1, 2 *]

[1] National Key Laboratory of Crop Genetic Improvement, Huazhong Agricultural University, Wuhan 430070, China

[2] Hubei Hongshan Laboratory, Huazhong Agricultural University, Wuhan 430070, China

[3] Yazhouwan National Laboratory, Sanya 572024, China

[4] Huanggang Academy of Agricultural Sciences, Huanggang 438000, Hubei, China

[5] Department of Root Biology and Symbiosis, Max Planck Institute of Molecular Plant Physiology, Potsdam-Golm, 14476, Germany

[§] These authors contributed equally to this work

[*] Corresponding author: yjianbing@mail.hzau.edu.cn

Abstract

Global food security requires sustainable strategies to improve crop yield and nutrition. Although thiamine pyrophosphate (TPP), the active form of vitamin B1, plays a central role in energy metabolism, redox homeostasis, and carbon assimilation, its contribution to crop yield and quality remains largely unexplored. Here, we show that *ZmTPK2*, a thiamine pyrophosphokinase encoded by the major ear length QTL *qKB6.2a*, is a key regulator of maize yield. We reveal that *ZmTPK2*-dependent TPP homeostasis synchronizes three cornerstones of plant metabolism: mitochondrial tricarboxylic acid (TCA) cycle activity, chloroplast-mediated carbon fixation, and nitrogen utilization. Both overexpression and knockout of *ZmTPK2* disrupt yield and grain quality, revealing that optimal TPP levels are required for productivity. Exogenous TPP supplementation increases grain yield in maize, rice, and rapeseed up to 9.8%. These findings identify TPP metabolism as a key regulatory pathway for metabolic engineering, biofortification, and global food security solutions.

Introduction

Global food security is increasingly threatened by climate change, extreme weather events, and rapid population growth. Achieving higher crop yields on limited arable land is a central goal of sustainable agriculture[1,2]. Maize (*Zea mays* L.), as one of the most widely cultivated cereal crops, serves as a key staple for both human consumption and livestock feed. Among its yield components, ear length is a critical determinant of grain productivity, as longer ears accommodate more florets and kernels, directly influencing final yield[3,4]. Thiamine pyrophosphate (TPP), the biologically active form of vitamin B1, serves as a vital metabolic coenzyme that regulates plant growth, energy homeostasis, and stress responses[5]. TPP-dependent enzymes are central to key metabolic pathways, including the pentose phosphate pathway (PPP), TCA, and Calvin-Benson cycles, which govern carbon assimilation, redox balance, and ATP production[6,7]. These pathways are essential for photosynthesis and mitochondrial respiration, directly impacting biomass accumulation, reproductive success, and grain filling[8]. However, the role of TPP-related genes in regulating grain yield and quality remains largely unexplored.

Regulatory variations are major determinants of gene expression diversity, playing a crucial role in shaping phenotypic traits in plants, particularly maize. Over 60% of maize QTLs are associated with regulatory variations[9], influencing key agronomic traits such as ear length[3,4,10], kernel row number (KRN)[11-13], kernel size[14-16], flowering time[17,18], stress tolerance[19-22], and environmental adaptation[23]. Recent advances in genome editing enable precise manipulation of regulatory elements, allowing fine-tuning of gene expression for improved crop performance[24,25]. Editing regulatory elements has successfully enhanced maize yield[10,26], tomato fruit size[24], and rice agronomic traits[27,28]. However, the optimal expression levels for individual genes and the intricate relationships between gene transcription levels and phenotypic outcomes remain largely unresolved.

In this study, we map the ear length QTL, *qKB6.2a*, and clone the underlying gene (*Zm00001d037916/ZmTPK2*), which encodes a thiamine pyrophosphokinase 2. We find that *ZmTPK2* regulates maize development and growth by modulating TPP levels, thereby influencing the canonical plant energy metabolism pathways, including pentose phosphate

(PPP) pathway, tricarboxylic acid (TCA) cycle, and Calvin-Benson cycle. Genetic analysis reveals that variations in *ZmTPK2* expression, driven by three single nucleotide polymorphisms (SNPs) and one insertion-deletion (InDel) in its promoter and cis-regulatory element (CRE), affect ear length. *ZmTPK2* transcription level has a dosage effect on maize ear length and productivity, with optimal expression maximizing ear length and grain yield. Additionally, exogenous treatment of 0.04% (w/v) TPP significantly enhances hybrid yields in maize, rice and rapeseed. These findings offer strategies for improving grain yield through manipulation of *ZmTPK2* expression and optimization of TPP levels.

Results

Map-based cloning of a major ear length QTL-*qKB6.2a*

We previously mapped eight ear length QTLs in the recombinant inbred lines (RILs) derived from the cross between KUI3 (short ear) and B77 (long ear)[29]. Among these QTLs, *qKB6.2,* located on chromosome 6, had the largest effect and accounted for 18.92% of ear length phenotypic variation[29] (Supplementary Fig. 1a). To clone *qKB6.2*, a heterogeneous inbred family (HZAU-551-1), which harbored a 5.2-Mb heterozygous region covering the candidate region, was selected from the F_6 generation[30], and self-pollinated to generate near-isogenic lines (NILs). Based on progeny test, *qKB6.2* was further separated into two independent QTLs, *qKB6.2a* and *qKB6.2b* (Supplementary Fig. 1b). Detailed analysis revealed that *qKB6.2a* had pleiotropic effects on ear traits (Fig. 1a-f), with $qKB6.2a^{B77}$ displaying increased inflorescence meristem (IM) length (175.2μm vs. 262.5μm, $P = 9.6\times10^{-27}$), and more florets per row (21.2 vs. 24.5, $P = 9.6\times10^{-7}$) on 3-4 mm developing ears comparing with those of $qKB6.2a^{KUI3}$, suggesting that the IM of $qKB6.2a^{B77}$ has a stronger ability to generate florets. Moreover, *qKB6.2a* did not affect flowering time, plant architecture or kernel related traits (Supplementary Fig. 2a-o). Similar pollination success rates were observed between $qKB6.2a^{B77}$ (~65.4%) and $qKB6.2a^{KUI3}$ (~66.7%) following pollination. However, $qKB6.2a^{B77}$ produced more florets, which results in increased kernel number per row (KNPR, 14.2 vs. 16, $P = 2.9\times10^{-6}$) by ~12.7% (Fig. 1e), ear length (9.8 cm vs. 10.5 cm, $P = 1.5\times10^{-5}$) by ~7.1% (Fig. 1f), and kernel weight per ear (27.8g vs. 30.3g, $P = 8.0\times10^{-4}$) by ~9.0% (Supplementary

Fig. 2p). Collectively, *qKB6.2a* enhances maize ear traits and grain yield by boosting floret production in ear primordia.

To identify the causal variant underlying *qKB6.2a*, we screened approximately 80,000 individuals and obtained seven new recombinants, with which we narrowed *qKB6.2a* to a ~ 58.2 kb (chr6: 141,874,245-141,932,398, B73 RefGen_v4) interval flanked by markers M5 and M7 (Fig. 1g). Homozygous recombinants with the $qKB6.2a^{B77}$ allele exhibited longer ears, increased KNPR, and higher ear weight, without changes in ear diameter (ED) and KRN across two environments (Supplementary Fig. 2q and Supplementary Table 1). This region contains two annotated genes, *Zm00001d037915* and *Zm00001d037916* (Fig. 1g), but only *Zm00001d037916* was differentially expressed in the developing ears of the NILs (Fig. 1h, i). In addition, no coding sequence variations were detected between the NILs for both genes (Fig. 1j, Supplementary Fig. 3a). *Zm00001d037916*, encoding thiamine pyrophosphokinase2 (TPK2), was identified as the candidate gene for *qKB6.2a* and is subsequently referred to as *ZmTPK2*. Sequencing revealed two SNPs in the promoter, and ten SNPs with one InDel in the intron region (Fig. 1j, Supplementary Table 2, Supplementary Data 1). Specifically, published chromatin interaction data showed a 983bp CRE (~41.8 kb upstream of *ZmTPK2*, chr6:141,888,459-141,889,441, RefGen_v4), within *qKB6.2a* QTL interval, physically interacts with its promoter (chr6:141,930,290-141,931,547, RefGen_v4) via a chromatin loop (Supplementary Fig. 3b, Supplementary Data 2)[31]. Both the CRE and promoter regions coincide with chromatin regions exhibiting open chromatin signatures, further supporting their potential regulatory activity[32] (Supplementary Fig. 3b). Sequencing of 1,724 bp region covering entire CRE identified one SNP and one InDel between the NILs (Fig. 1j, Supplementary Table 2, Supplementary Data 1). Taken together, these sequence changes in the promoter and CRE region were likely responsible for *ZmTPK2* differential expression and were thus proposed as the causal variants underlying *qKB6.2a*.

Variants in the *ZmTPK2* promoter and CRE independently contribute to the ear length variation

To confirm the causal variants, we analyzed firefly luciferase (LUC) activity driven by the

different *ZmTPK2* promoters and CRE alleles in maize protoplasts. LUC driven by promoters from *qKB6.2a*^{KUI3} (*pZmTPK2*^{KUI3}) had much lower activity than that from *qKB6.2a*^{B77} (*pZmTPK2*^{B77}). Importantly, CRE from *qKB6.2a*^{KUI3} (*creZmTPK2*^{KUI3}) significantly increased the expression of *pZmTPK2*^{KUI3}-driven *LUC*, but CRE from *qKB6.2a*^{B77} (*creZmTPK2*^{B77}) had a slight effect on the expression of *pZmTPK2*^{B77}-driven *LUC* (Fig. 1k, Supplementary Fig. 3c). These results align with the observation that *ZmTPK2* expression levels in *qKB6.2a*^{KUI3} are higher than in *qKB6.2a*^{B77}, suggesting that *creZmTPK2*^{KUI3} acts as an enhancer for *ZmTPK2* expression, and that the promoter and CRE variations jointly contribute to gene expression differences. Further, point mutations, which resulted in substitution of C with T or A with G at site -362 and -480 respectively, in *pZmTPK2*^{KUI3} significantly elevated the promoter activity, with T and G alleles being favorable (Fig. 1k, Supplementary Fig. 3c). Similarly, substitution of T with C or insertion of AAAAT in *creZmTPK2*^{B77} increased the LUC activity driven by *pZmTPK2*^{B77} (Fig. 1k, Supplementary Fig. 3c), indicating that the C allele and AAAAT insertion elevated enhancer activity. Collectively, these variations in promoter and CRE of *ZmTPK2* may contribute to differences in gene expression and ear length variation.

We investigated the genotypic data of two causal SNPs in *ZmTPK2* promoter using a diverse association population panel from published data[33], and genotyped the SNP and the InDel within *ZmTPK2* CRE among 201 diverse maize inbred lines (Supplementary Data 3) in the same population with Kompetitive Allele-Specific PCR (KASP)[34]. Four distinct haplotypes were identified (Fig. 1l), with the haplotype *Hap1* being detected only in B77 (one of the QTL parents) (Fig. 1m). Further genotyping of 54 teosinte samples and 143 landrace accessions revealed that teosintes only carried *Hap2* and *Hap4*, while landraces harbored *Hap2*, *Hap3* and *Hap4*. *Hap1* was absent in both teosintes and landraces (Fig. 1m). These results suggest that *Hap1* likely arose through a natural mutation event in modern maize and highlight its significant potential for improving grain yield by incorporating this favorable allele into breeding programs.

Optimized expression of *ZmTPK2* is critical to increase ear length and yield

To confirm the role of *ZmTPK2* in ear length regulation, we created two CRISPR-Cas9

knockout lines (*tpk2-cr1* and *cr2*, Supplementary Fig. 4a). The *tpk2-cr1* mutant carries a 218-bp deletion in exon1 and intron1, deleting 35 amino acids, while the *tpk2-cr2* mutant has a 1-bp deletion in exon1 and a 2-bp deletion in exon2, causing a frameshift mutation. Both mutants had smaller plant architecture and ears, with reductions in ear length (0.43-0.84 cm), KNPR (1.29-1.45), and ear weight (EW, 6.80-13.61 g) compared to non-transgenic (NT) siblings (Fig. 2a-e). Moreover, both mutants showed reductions in other agronomic and kernel traits, excluding flowering time across multiple environments (Supplementary Fig. 4b-p and 5). Developing ear analysis revealed decreased IM size and fewer floret numbers per row in *tpk2-cr1*, consistent with the effects of the short ear allele $qKB6.2a^{KUI3}$ (Supplementary Fig. 6). These results confirmed the role of *ZmTPK2* in regulating ear length and yield.

We developed seven overexpression (OE) lines (*TPK2-OE1~7*) with *ZmTPK2* expression driven by the ubiquitin promoter. All OE lines had enhanced plant height with variable ear phenotype (Fig. 2f-j, Supplementary Fig. 7a-d). However, *TPK2-OE2~4* plants appeared to have optimal expression level (~10.3-18.7) in that they displayed significant increases in ear length, KNPR, KRN and kernel weight per ear. By contrast, *TPK2-OE1* (~6.8) showed reduced ear length, and KNPR with weakly negatively affected KRN and kernel weight per ear, while excessive expression in *TPK2-OE6~7* (~25.9-29.6) resulted in significant decreases in ear length, KNPR and kernel weight per ear without affecting KRN. In addition, *TPK2-OE5* lines (~ 21.6) had no effect on ear traits. The IM length was increased in *TPK2-OE2*~3, corresponding to longer ears, and decreased in *TPK2-OE6~7*, consistent with shorter ears (Supplementary Fig. 7e, f). Similar changes of these overexpression lines were observed in a second field season (Supplementary Fig. 8). These findings suggest that fine-tuned regulation of *ZmTPK2* expression is critical for optimizing maize ear length and yield by promoting balanced ear development.

To explore the relationship between *ZmTPK2* expression and ear length in a natural population, we analyzed *ZmTPK2* expression levels in 55 maize developing ears across various haplotypes. The favorable haplotype *Hap1* (B77) had comparable expression level of *ZmTPK2* to *TPK2-OE2*, while the *Hap2* and *Hap4* had lower expression levels (2.45, and 1.82, respectively),

similar to those of non-transgenic lines. *Hap3* had progressively higher expression level, resembling *TPK2-OE4~5*(Fig. 2k). *Hap1* plants displayed longer ear than *Hap2*, *Hap3*, and *Hap4* (Fig. 2l), though statistical significance was limited by the small *Hap1* sample size. These results suggested that natural variation of *ZmTPK2* precisely regulates *ZmTPK2* expression levels, with most maize inbred lines in natural populations failing to achieve the optimal expression necessary for maximal ear length (Fig. 2m). This finding highlights the considerable potential for genetic improvement of ear length in maize.

ZmTPK2 regulates thiamine pyrophosphate biosynthesis

ZmTPK2 is broadly expressed in maize tissues, with the highest levels in developing ears and meristems. Expression differences between $qKB6.2a^{KUI3}$ and $qKB6.2a^{B77}$ were specific to developing ears and inflorescence meristems, driving phenotypic variations in NIL ear traits (Fig. 1a-f, Supplementary Fig. 9a). Thiamine pyrophosphokinase (TPK) functions in the conversion of thiamine to TPP in the cytosol, which is conserved across plant species[5] (Fig. 3a). We found that ZmTPK2 protein was localized in the cytosol (Supplementary Fig. 9b). *In vitro* assays using purified ZmTPK2 confirmed its enzymatic activity, showing TPP production increased with thiamine concentrations up to 150μM, with a Michaelis constant (K_m) of 15.57 μM, while as anticipated the negative control showed no activity (Fig. 3b). These results verify ZmTPK2 as a critical enzyme for TPP synthesis in the maize cytosol.

To investigate whether *ZmTPK2* regulates TPP biosynthesis *in vivo*, we next measured TPP levels in developing ears and leaves. TPP levels in developing ear were significantly higher in the longer ear $qKB6.2a^{B77}$ lines than that in $qKB6.2a^{KUI}$ lines, with insignificant change in leaves (Supplementary Fig. 10a). Similarly, *tpk2-cr1* mutants and *TPK2-OE6~7* plants with shorter ears had reduced TPP levels, whereas *TPK-OE1*, *2* and *4* plants with longer ears showed increased TPP levels in developing ears and leaves (Fig. 3c-e). These results confirm that ZmTPK2 catalyzes the conversion of thiamine into TPP *in vivo*, with higher TPP levels being essential for longer ears. To test if exogenous TPP could rescue shorter ears in *tpk2-cr1*, we sprayed *tpk2-cr1* plants with 0.02%, 0.04% and 0.06% TPP solutions (w/v) 30 days post-sowing, during female inflorescence meristem development. All treatments significantly

increased ear length, with complete rescue of the mutant phenotype (Fig. 3f, g, Supplementary Fig. 10b, c). Taken together, these results suggest that *ZmTPK2* regulated ear length by modulating TPP levels, and that exogenous TPP application can fully rescue the shorter ear phenotype exhibited by the *tpk2-cr1* mutations.

***ZmTPK2* participates in energy pathways to regulate kernel quality**

TPP is a vital coenzyme for enzyme complexes such as pyruvate dehydrogenase (PDH) and α-ketoglutarate dehydrogenase in the TCA cycle, as well as transketolase (TK) in the PPP and Calvin-Benson cycle, all of which are essential for photosynthesis and respiration[6,35]. To investigate whether *ZmTPK2* affects these processes, we measured net photosynthetic and respiratory rates in *tpk2-cr1*, *TPK2-OE* (*OE1*, *OE2*, *OE4* and *OE7*) plants. Compared to NT, *tpk2-cr1* mutants, and *TPK2-OE7* lines exhibited significantly reduced photosynthetic and respiratory rates, whereas *TPK2-OE1*, *OE2*, *OE4* plants showed increased photosynthetic and respiratory rates (Fig. 3h-k). To further probe the underlying metabolic change, we performed an energy metabolomic analysis on the leaves of *tpk2-cr1* mutants and *TPK2-OE2* and *TPK2-OE7* overexpression lines. Our results revealed substantial disruptions in core metabolic pathways, including the TCA, PPP, and Calvin-Benson cycles. Specifically, *tpk2-cr1* and *TPK2-OE7* plants exhibited reduced levels of key intermediates such as pyruvate, acetyl-CoA, α-ketoglutarate, malate, lactate, fructose-6-phosphate, 6-phosphogluconate, and ribulose-5-phosphate (Supplementary Fig. 11 and 12), whereas *TPK2-OE2* plants displayed an overall increase in these metabolites (Supplementary Fig. 13), consistent with their enhanced photosynthetic and respiratory rates.

Enhanced photosynthesis drives greater carbon assimilation in leaves, and facilitates sugar transport to developing kernels, thereby supporting starch and protein biosynthesis, as well as nitrogen metabolism[8,36]. To elucidate the impact of *ZmTPK2* on kernel quality, we conducted metabolomic, starch, and protein analyses on mature kernels of *tpk2-cr1* mutants, *TPK2-OE2* and *TPK2-OE7* overexpression lines. In *tpk2-cr1* lines, levels of key sugars (sucrose, glucose, and fructose), essential amino acids (methionine, tryptophan, and threonine), and total protein content were all significantly reduced, (Fig. 3l, m, Supplementary Fig. 14 and 15), while starch

content was invariant (Fig. 3n). In contrast, for the overexpression materials, *TPK2-OE2* plants with moderately elevated *ZmTPK2* expression exhibited increased accumulation of sugars and amino acids, resulting in a ~1.1% increase in grain protein content but a slight decrease in starch content (Fig. 3o-q, Supplementary Fig. 15). Conversely, *TPK2-OE7* plants with excessively high *ZmTPK2* expression showed reduced sugar and amino acid levels, along with lower protein and starch contents (Fig. 3o-q, Supplementary Fig. 15). Based on these findings, we propose a model in which appropriately tuned *ZmTPK2* expression promotes optimal TPP production, thereby enhancing the activity of key metabolic pathways such as the TCA and Calvin-Benson cycles. This supports robust photosynthesis, respiration, and nitrogen assimilation, ultimately boosting yield and protein content. However, when *ZmTPK2* expression is either too low (as in *tpk2-cr1*) or excessively high (as in *TPK2-OE7*), the resulting imbalance in TPP levels disrupt energy metabolism, leading to reduced efficiency of the TCA and Calvin cycles, and consequently, decreased yield and nutritional value (Fig. 3r).

Natural favorable haplotype of *ZmTPK2* enhances grain yield

Maize grain yield is a complex trait governed by numerous QTLs[29,37], with some exhibiting significant effects only in specific genetic backgrounds, thereby limiting their boarder application in breeding. To evaluate the breeding potential of *ZmTPK2* in hybrids, 41 founder inbred lines were genotyped using four KASP markers. Among these, 37 lines carried *Hap4*; four carried *Hap2* (Supplementary Table 3), while the favorable haplotype *Hap1* was absent, highlighting its untapped potential in commercial breeding. We crossed $qKB6.2a^{KUI3}$ and $qKB6.2a^{B77}$ directly with four elite maize inbred lines (one *Hap2* and three *Hap4* carriers) to generate F1 hybrids. The hybrids derived from $qKB6.2a^{B77}$exhibited superior performance, with a 4.3%-8.7% increase in ear length and a corresponding 7.4%-14.2% enhancement in grain yield compared to those derived from $qKB6.2a^{KUI3}$ lines (Fig. 4a-d) under a planting density of 67,500 plants per hectare. While longer ear can sometimes result in thinner cobs, increased KNPR with no adverse changes in ED were observed in PH4CV and Jing92 backgrounds, and a significant ED increase was seen in Zheng58 and V76-1 backgrounds (Fig. 4e, f). Hybrids derived from $qKB6.2a^{B77}$ also demonstrated lower *ZmTPK2* expression levels than those derived from $qKB6.2a^{KUI3}$, which were correlated with an increased ear length and grain yield,

consistent with observations in the NILs (Fig. 4g). Repeated field experiments in Xiangyang, Hubei confirmed these outcomes (Supplementary Fig. 16). In summary, the natural *Hap1* allele enhances ear length, KNPR, and consequently maize grain yield through regulating *ZmTPK2* expression levels, demonstrating its significant potential for hybrid breeding and genetic improvement.

The application of TPP greatly increases yield in multiple plant species

We have demonstrated that the application of a 0.04% TPP solution successfully restored reduced ear length in *zmtpk2-cr1* mutants (Fig. 3f, g). In our experiments, we evaluated the effect of foliar application of 0.04% TPP on NILs carrying either the *Hap1* allele (characterized by lower *ZmTPK2* expression and higher endogenous TPP levels) or the *Hap3* allele (characterized by higher *ZmTPK2* expression and lower endogenous TPP levels). TPP treatment increased ear length and yield-related traits in both NIL backgrounds (Supplementary Fig. 17). Furthermore, maize founder inbred lines carrying *Hap2* and *Hap4* alleles exhibited relatively low *ZmTPK2* expression levels, likely leading to insufficient TPP accumulation. These findings suggest that endogenous TPP levels in maize potentially have not reached an optimal threshold, and that external TPP applications could potentially improve ear length and grain yield. To further investigate the efficacy of TPP, we evaluated four widely cultivated maize hybrids in China: Jingke968, Zhengdan958, Qiyu58, and Dedan5. Jingke968, and Zhengdan958, *Hap2/Hap4* heterozygous hybrids, are among the top five most cultivated hybrids in China over the past decade, with cumulative planting areas of 1.09 and 0.70 million hectares, respectively (Data from National Agro-Tech Extention and Service Center, https://www.natesc.org.cn/). Qiyu58 (*Hap4/Hap4*) and Dedan5 (*Hap2/Hap2*), regionally promoted hybrids, were included to evaluate TPP's effectiveness across different genetic backgrounds. All hybrids were grown under standard practices at a density of 67,500 plants per hectare and treated with a 0.04% TPP solution 30 days after sowing. The treatment significantly increased ear length by 0.42 - 1.15 cm and plot yield by 4.5% - 7.1% (429.4 - 675.0 kg/ha) compared to controls, with minimal effects on ear diameter and plant architecture across multiple environments (Fig. 5a-c, Supplementary Fig. 18 and 19a-g).

In rice, TPP treatment similarly demonstrated significant yield benefits. Huanghuazhan, China's most widely cultivated indica rice variety, is highly regarded for its superior yield potential, grain quality, and economic contributions. In addition to Huanghuazhan, three regionally promoted hybrid varieties - Xinliangyou9100, Taiyou398, and Huangliangyou913 - were evaluated to examine TPP's effectiveness across diverse backgrounds treatment with a 0.04% TPP solution resulted in significant increases in grain size and yield, with improvements of 6.7% - 9.8% (633.3 - 866.7 kg/ha) compared to controls. These results were consistent across all varieties grown at a density of 300,000 plants per hectare, reflecting standard farmer practices in China (Fig. 5d, e, Supplementary Fig. 19h-j and 20). Similarly, we observed similar benefits in two economically significant hybrids: Qingyou8 among the top ten rapeseed varieties in terms of cultivation area and Zhongyouza501 with higher oil content. TPP application significantly enhanced silique length (0.35 - 0.63cm), seed size (0.14 - 0.17 mm^2), and thousand-seed weight (0.25 - 0.41g) in both hybrids, with no changes in plant height or oil content (Fig. 5f-j). Collectively, these results demonstrate that external TPP supplementation enhances yield-related traits in maize, rice, and rapeseed across elite varieties under actual field cultivation conditions and planting densities. This underscores its potential as a valuable tool for improving crop productivity in sustainable agriculture.

Discussion

Thiamine pyrophosphate (TPP), the active form of vitamin B1, is an essential coenzyme that regulates key metabolic pathways, including the PPP, TCA, and the Calvin-Benson cycles[7]. While plants are known to synthesize thiamine de novo[38] - primarily in plastids (chloroplasts) with subsequent phosphorylation in the cytoplasm to form TPP - it is generally believed that thiamine is synthesized in leaves and transported to developing sink tissues, such as ears, to support carbohydrate metabolism and cellular growth[7,39]. Here, we identified *ZmTPK2*, a thiamine pyrophosphokinase, as a key regulator of inflorescence meristem (IM) size, floret number, ear length, and grain yield, acting through modulation of TPP levels (Figs. 1-3). Our findings supplement the classical model of thiamine metabolism by demonstrating that developing maize ears can locally synthesize thiamine. RNA-seq analysis of 2-5 mm immature

maize ears in NILs revealed the expression of key thiamine biosynthesis genes (*Thi1*, *Thi2*, *THIC*, *TH1*, and *HETK*), indicating that thiamine biosynthesis is not solely leaf-derived but occurs within young ears to support early developmental processes (Supplementary Table 4). This discovery aligns with prior studies[40,41], and provides a mechanistic explanation for ear length variation among NILs, which correlates with differential *ZmTPK2* expression and localized TPP accumulation. Despite comparable *ZmTPK2* expression and TPP content in leaves, ear length variation was primarily attributed to spatiotemporal differences in *ZmTPK2* expression during early ear development, underscoring the localized regulation of TPP metabolism in shaping growth trajectories.

Interestingly, we observed a non-linear trend in TPP accumulation with increasing *ZmTPK*2 expression - an initial increase followed by a decline. This suggests a feedback regulatory mechanism, potentially mediated by the TPP riboswitch. It, a cis-regulatory RNA element in the 3' UTR of *THIC* mRNA, modulates gene expression in response to intracellular TPP levels. At low TPP concentrations, it promotes proper splicing, increasing *THIC* expression and TPP biosynthesis. Conversely, at high TPP levels, a conformational shift induces aberrant splicing or mRNA degradation, reducing *THIC* expression and thereby limiting further TPP accumulation[6]. We propose that *ZmTPK2* overexpression initially drives TPP biosynthesis, but as TPP accumulates, riboswitch-mediated repression of *THIC* reduces its biosynthesis, leading to the observed decline. This aligns with findings in Arabidopsis, where the TPP riboswitch plays a critical role in maintaining TPP homeostasis. To validate this hypothesis, future studies should: (i) characterize the *ZmTHIC* 3' UTR structure to confirm riboswitch-mediated regulation, (ii) employ CRISPR-Cas9 to disrupt riboswitch elements and assess its impact on TPP dynamics, (iii) perform RNA quantification and ribosome profiling to investigate splicing and translational regulation under varying TPP conditions.

Beyond its role in plant development, TPP also plays a crucial role in enhancing resilience against biotic and abiotic stresses[7]. Increasing TPP synthesis through genetic engineering presents a promising strategy for improving crop productivity and stress tolerance. CRISPR/Cas9 technology has been successfully utilized for precision breeding, particularly by modifying regulatory regions of key genes to enhance agronomic traits[24-26]. In maize, *ZmTPK2*

358 expression is regulated by variations in CREs and promoter regions, which in turn influence
359 ear length. Our findings suggest that an optimal balance of *ZmTPK2* expression is required to
360 achieve ideal ear development (Fig. 2). This provides an opportunity for targeted genome
361 editing of *ZmTPK2* regulatory regions to fine-tune expression, thereby optimizing ear
362 architecture and potentially improving grain yield and quality. Moreover, the favorable
363 *ZmTPK2* haplotype *Hap1*, currently confined to the B77 inbred line and absent in widely used
364 founder lines, represents a valuable yet underutilized resource for maize breeding. Marker-
365 assisted backcrossing could facilitate the introgression of *Hap1* into elite germplasm,
366 enhancing yield potential and agronomic performance. Beyond its agronomic significance, TPP
367 is essential for human and animal health, playing key roles in nervous system function, insulin
368 sensitivity, and energy metabolism[42,43]. Its increasing use as a dietary supplement highlights
369 the potential for biofortification. Integrating the complete TPP biosynthetic pathway into crop
370 kernels through synthetic biology could elevate endogenous TPP levels, addressing nutritional
371 deficiencies and promoting health benefits.
372
373 Exogenous TPP applications have demonstrated potential in improving crop productivity, as
374 shown by foliar sprays (e.g., 0.04% w/v) in maize, rice, and rapeseed (Fig. 5). This finding
375 highlights a broader potential of metabolic cofactors in enhancing agricultural performance.
376 Although our foliar TPP application experiments demonstrated consistent yield enhancement
377 across multiple crops, direct mechanistic validation remains technically challenging.
378 Quantitative tracing of exogenous TPP uptake, transport, and intracellular conversion is limited
379 by the lack of stable isotopic or fluorescent probes, as TPP is highly polar and rapidly
380 hydrolyzed in planta. Moreover, current analytical approaches do not allow spatiotemporal
381 resolution of TPP dynamics at the cellular level, and tissue-specific manipulation of thiamine
382 metabolism genes in major crops such as maize remains labor-intensive. These challenges
383 collectively constrain definitive tests of the causal mechanisms underlying TPP-mediated yield
384 improvement, which will require future methodological advances. One particularly important,
385 yet underexplored, aspect of thiamine metabolism involves the transport of TPP across cellular
386 compartments. Mitochondrial TPP transporters, identified in yeast, humans, and Drosophila,
387 belong to the mitochondrial carrier family (MCF). While MCF proteins primarily localize to

the inner mitochondrial membrane, some also function in chloroplasts and peroxisomes[44]. Understanding TPP transport mechanisms in plants could provide insight into its role in mitochondrial metabolism and overall crop performance. To investigate potential TPP transporters in maize, we employed AI-driven protein structure prediction using AlphaFold[45]. A genome-wide structural analysis identified 10 MCF proteins through Gene Ontology (GO) annotation, among which two candidates (Zm0001d011226 and Zm00001d042213) received high-confidence scores as potential TPP transporters (Supplementary Table 5). These findings lay the groundwork for future functional studies to elucidate their role in TPP translocation and mitochondrial metabolism.

From an agricultural perspective, TPP is non-toxic and environmentally safe, making it an attractive candidate for external applications, including drone-based delivery. However, its instability and high production costs present challenges for large-scale use. Addressing these issues requires the development of stable, cost-effective TPP analogs with retained bioactivity. Advances in synthetic biology offer promising avenues for improving TPP biosynthesis, potentially lowering production costs. Additionally, optimizing application strategies - including dosage, timing, and delivery methods - will be crucial for ensuring economic feasibility and environmental sustainability. Integrating these approaches could unlock the full potential of TPP and its derivatives as tools for enhancing crop productivity, offering a sustainable solution to global food security challenges.

Methods

QTL mapping and transgenic validation of *ZmTPK2*

To fine-map *qKB6.2a* locus, a heterogeneous inbred family (HIF), designated HZAU-551-1[30], was used. The HIF individuals were heterozygous only in the *qKB6.2a* region, with the rest of the genetic background being homozygous. These individuals were self-pollinated to generate recombinant inbred lines, which were further self-pollinated to produce homozygous progeny for the $qKB6.2a^{KUI3}$ and $qKB6.2a^{B77}$ alleles. The plants were grown in fields in Hainan (Sanya; 18.3°N, 109.5°E) and Hebei (Baoding; 38.5°N, 115.3°E), in 2.5m rows spaced 0.5 m apart, with 11 plants per row. Progeny testing was conducted by comparing ear length between

homozygous families derived from each recombinant line. One-way analysis of variance (ANOVA) was performed in Microsoft Excel to assess significant difference in ear length, and then refine the QTL interval. All QTL mapping markers are listed in Supplementary Table 6.

To investigate the function of *ZmTPK2*, we performed CRISPR-Cas9-based gene editing and overexpression experiments. Two guide RNAs targeting the first and second exons of *ZmTPK2* were designed and inserted into the pCPBZmUbi-hspCas9 vector[46,47]. We also fused *ZmTPK2* with yellow fluorescent protein and overexpressed it with the ubiquitin promoter. Both the CRISPR-Cas9 and overexpression constructs were introduced into the maize inbred line KN5585[48] via Agrobacterium-mediated transformation at Weimi Biotechnology (Jiangsu, China). Transgenic plants were validated using RT-qPCR for overexpression lines and sequencing for CRISPR-Cas9 editing events. The primers used for validation are listed in Supplementary Table 7. Transgenic lines were grown in field trials conducted at three locations in China: Gongzhuling, Jilin (43.5° N, 124.82° E), Zhangye, Gansu, (38.9° N, 100.5° E), and (Huanggang, Hubei (30.58° N, 114.31° E). The plants were cultivated in 2.5 m rows spaced 0.5 m apart, with 11 individuals per row. Progeny tests were conducted to evaluate phenotypic differences, and statistical analysis was performed using one-way ANOVA.

Expression quantification of *ZmTPK2* and RNA-seq analysis

To quantify the expression of *ZmTPK2* (*Zm00001d037916*) and perform RNA-seq analysis, total RNA was extracted from various tissues of two NILs, including mature leaves, internode, bract, developing tassel, developing ear (< 2mm, 2-5mm, and 5-8mm), inflorescence meristems and spikelet pair meristems. RNA was also performed using the Quick RNA Isolation Kit (Huayueyang Biotechnology CO., LTD. Beijing, China). Genomic DNA contamination was removed from the extracted RNA using the EasyScript One-Step gDNA Removal Kit (TransGen Biotech). First-strand complementary DNA (cDNA) synthesis was carried out using the cDNA Synthesis SuperMix (TransGen Biotech). Real-time fluorescence quantitative PCR (qPCR) was conducted using SYBR Green Master Mix (Vazyme Biotech) on a CFX96 Real-Time System (Bio-Rad) to quantify *ZmTPK2* expression. The relative expression levels were calculated using the ($2^{-\Delta\Delta CT}$) method[49], with *ZmACTIN* (*Zm00001d010159*) serving as the

internal control. All experiments were performed in three biological replicates. Primers used for qPCR are listed in Supplementary Table 7.

For RNA-seq analysis, RNA, extracted from < 2 mm developing ears of the NILs, was used. Three biological replicates were prepared for each sample. RNA library preparation was performed using the TruSeq Stranded mRNA LT-SetA (RS-122-1201, Illumina), and sequencing was conducted using the HiSeq X-Ten platform. Raw sequecing reads were quality-checked and filtered using Trimmomatic (v0.36) to remove lower-quality reads[50]. The filtered reads were aligned to the B73 v4 reference genome using RSEM-1.3.0 with default parameters, and gene expression levels were estimated[51].

LUC activity assay

To evaluate the effect of variations in the CRE and promoter region of *Zm00001d037916* on gene expression, a dual-luciferase (LUC) transient expression assay was performed in maize protoplasts. Based on the Oh43 reference genome, we successfully amplified a 1,190 bp CRE region and a 1,724 bp promoter region from NILs carrying $qKB6.2a^{KUI3}$ and $qKB6.2a^{B77}$, respectively (Supplementary Data 1). To improve protoplast transformation efficiency and avoid issues associated with large vector constructs, we subcloned 945 bp of the CRE and 642 bp of the promoter region - each containing all identified polymorphic sites - into the pGreenII 0800-LUC reporter vector upstream of the mini-Cauliflower Mosaic Virus *35S* (*mpCaMV*) promoter. Primer sequences are listed in Supplementary Table 7. Point mutation sequences were synthesized in TSINGKE Biological Technology. All eight sequence variants used for reporter constructs are detailed in Supplementary Data 1. Protoplasts were isolated from the leaves of 10-day-old etiolated B73 seedlings. Polyethylene glycol (PEG)-mediated transformation was used to introduce the plasmids into the protoplasts[52]. Following transformation, both firefly LUC and Renilla (REN) LUC activities were measured using the Dual-Luciferase Reporter Assay System (Promega, Madison, WI, USA) according to the manufacturer's protocol (https://www.promega.com/resources). Relative LUC activity was calculated by normalizing firefly LUC activity to Renilla LUC activity. Each construct was analyzed in three technical replicates across three to six biological replicates.

Measurement of photosynthetic and respiratory rate

Net photosynthetic and respiratory rate were measured on fully-expanded maize leaves using a portable gas exchange system (LI-6400XT, LI-COR Inc., USA)[53]. For net photosynthetic rate measurements, leaves were assessed under an ambient CO_2 concentration of 400 μmol mol^{-1} with a light intensity of 2000 μmol m^{-2} s^{-1} at light saturation, between 9 am and 11:30 am. Net respiratory rates were measured in the evening, between 8:00 pm and 10:30 pm, under an ambient CO_2 concentration of 400 μmol mol^{-1} and a light intensity of 0 μmol m^{-2} s^{-1}. Measurements were conducted at the v11-12 leaf stage on *zmtpk2-cr1*, *TPK2-OE2*, *TPK2-OE7* and non-transgenic control plants. Statistical differences between the groups were assessed using one-way ANOVA in Microsoft Excel, with significance determined at $P \leq 0.05$.

Endogenous TPP measurement

To measure endogenous TPP levels, we collected 2-5 mm developing ears and leaves (at the v11-v12 stage) from NILs, *zmtpk2-cr1* mutants, *ZmTPK2* overexpression lines, and their respective controls. Each group included three biological replicates. The collected samples were immediately frozen in liquid nitrogen, ground into powder, and stored at -80°C until further analysis. TPP metabolite content was analyzed by MetWare (http://www.metware.cn/). For extraction, 0.02 g of each sample was mixed with 200 μL of 70% (v/v) methanol. The mixture was vortexed for 5 minutes at 700 × g, allowed to stand on ice for 5 minutes, and this process was repeated twice. The samples were centrifuged at 16,100 × g for 10 minutes at 4°C. The supernatant was kept at 4°C overnight, followed by a second centrifugation under the same conditions. After centrifugation, 100 μL of the supernatant was collected for liquid chromatography-mass spectrometry (LC-MS) analysis. The metabolite extracts were analyzed using an LC-ESI-MS/MS system consisting of a UPLC system (ExionLC AD, https://sciex.com.cn/) coupled to a triple quadrupole mass spectrometer (Applied Biosystems 6500, https://sciex.com.cn/). Standard operating procedures were followed for data acquisition and metabolite quantification[54].

Measurement of metabolomics, starch and protein content

For energy metabolomics, fresh leaves (at the v11-v12 stage) were harvested from *zmtpk2-cr1* mutants, *TPK2-OE2, TPK2-OE7* and their respective controls, with three biological replicates per group. The samples were immediately frozen in liquid nitrogen and stored at -80°C until analysis. Energy metabolite profiling was performed by MetWare (http://www.metware.cn/). For metabolite extraction, 0.05 g of each sample was thawed, ground, and mixed with 500 μL of 70% (v/v) methanol. The mixture was vortexed for 3 minutes at 700 × g and centrifuged at 16,100 × g for 10 minutes at 4°C. A 300 μL aliquot of the supernatant was transferred to a new centrifuge tube and stored at -20°C for 30 minutes. The supernatant was then centrifuged again at 16,100 × g for 10 minutes at 4°C. A 200 μL aliquot of the clarified supernatant was passed through a Protein Precipitation Plate for subsequent LC-MS analysis Energy metabolites were analyzed using an AB Sciex QTRAP 6500 LC-MS/MS platform, consisting of a UPLC system (ExionLTM AD, https://sciex.com.cn/) coupled to a triple quadrupole mass spectrometer (Applied Biosystems 6500, https://sciex.com.cn/). Standard protocols were followed for LC-MS/MS data acquisition and metabolite quantification[55,56].

For sugar and amino acid metabolomics, mature kernels from *zmtpk2-cr1* mutants, *TPK2-OE2*, *TPK2-OE7*, and their respective controls were collected, with five biological replicates per group. Primary metabolites were extracted following a previously described protocol[57]. Briefly, 50 mg of kernel powder was extracted with 1 ml methanol: methyl-tertiary-butyl ether (MTBE) (1:3, v/v). A 300-μL aliquot from the lower polar phase was dried in a SpeedVac concentrator (without heating), derivatized with N-methyl-N-(trimethylsilyl) trifluoroacetamide (MSTFA), and analyzed by GC-MS (7890A-5975C, Agilent) as per established methods. One microliter of each sample was injected at 270°C in split mode (50:1) using helium (>99.999% purity) as the carrier gas at a 1 mL/min flow rate. Metabolites were separated on a DB-35MS UI capillary column (30 m × 0.25 mm, 0.25 μm) under the following temperature program: 90°C for 4 min, ramped at 8°C/min to 205°C (held for 2 min), then at 15°C/min to 310°C (held for 2 min). The transfer line and ion source temperatures were set to 300°C and 230°C, respectively, with a mass range of *m/z* 85-700. Metabolomic data were processed using Agilent MassHunter Qualitative (vB06.00) and Quantitative Analysis (vB.07.01) software. Metabolites were identified using the NIST library and an in-house database established with authentic

standards[58].

For total nitrogen content analysis in maize kernels, samples were first dried to a constant weight at 65 °C and then finely ground using a Tissuelyser-48 grinder (Shanghai Jingxin Industrial Development; 60 Hz, 60 s). A total of 90 - 110 mg of the powdered sample was wrapped in tin foil for testing. Nitrogen content was determined using a Dumas rapid nitrogen analyzer (Elementar). Prior to each measurement session, three standard asparagine samples were weighed as internal controls to ensure accuracy. After calibrating the instrument, sample weights were entered into the rapid N exceed software (EAS rapid N exceed), and the prepared samples were sequentially loaded into the sample chamberThe system automatically introduced each sample into the combustion tube for analysis. A total of 60 samples were processed per measurement cycle, and the resulting data were exported in Excel format for further analysis.

For starch content determination, 0.5 g maize kernel powder (denoted as m_1) was transferred to a clean, dry 25 mL volumetric flask. A total of 10 mL of 0.31 M hydrochloric acid (HCl) was added in two steps: 5 mL initially, followed by vigorous shaking to obtain a homogeneous suspension, and then the remaining 5 mL. The flask was submerged in a boiling water bath. During the first 3 minutes, the flask was shaken continuously to prevent clumping and ensure uniform hydrolysis. After 15 minutes of boiling, the flask was removed and immediately treated with 6 mL of ice-cold water (≤ 10 °C). The contents were mixed and cooled under running tap water to approximately 20 °C. Next, 1 mL of potassium ferrocyanide solution was added and mixed for 1 minute, followed by 1 mL of zinc acetate solution, with an additional 1-minute mixing. The volume was then brought up to 25 mL with distilled water, thoroughly mixed, and filtered. The initial filtrate (~first few milliliters) was discarded. The optical rotation (α_1) of the clear filtrate was measured using a polarimeter. The starch content was calculated using the following formula:

$$\text{Starch content (\%)} = (\alpha_1 \times F) / m_1 \quad \textbf{(1)}$$

where α_1 is the optical rotation (degrees), F is a starch factor (constant based on calibration),

and m_1 is the sample weight in grams.

In vitro ZmTPK2 activity assays

The coding sequence of *ZmTPK2* was cloned into the pET28a vector and transformed into the *E. coli* Rosetta strain. Cultures were grown at 37°C to an OD600 of 0.6, cooled to 28°C, and induced with isopropyl β-D-1-thiogalactopyranoside (IPTG) at a final concentration of 0.2 mM. Induced cultures were grown for an additional 12-16 hours at 28°C[59]. His-tagged ZmTPK2 protein was purified using the Ni-NTA protein purification system (QIAGEN) according to the manufacturer's protocol. Protein purity and concentration were evaluated using SDS-PAGE. The ZmTPK2 activity assay was performed in a reaction mixture (500 μL) containing 50 mM phosphate buffer (pH 8.0), 50 μM thiamine, 25 mM $MgCl_2$, 20 mM ATP, and 1 μg of purified ZmTPK2 protein. The reaction mixture was incubated at 37°C for 1 hour and terminated by the addition of 30% (w/v) trichloroacetic acid (TChlA) to achieve a final concentration of 2%. Thiamine concentrations ranging from 0 to 200 μM were used to determine reaction rates for k_m calculations[59,60]. The supernatant was analyzed for thiamine pyrophosphate (TPP) formation using HPLC, following the method described in the endogenous TPP measurement section. All assays were performed in three technical replicates to ensure accuracy.

Evaluation of grain yield-related traits

A total of four inbred lines, including one Hap2 line and three Hap4 lines, were selected based on genotyping and crossed with both $qKB6.2a^{KUI3}$ and $qKB6.2a^{B77}$, respectively. The resulting eight hybrids were grown during the 2023 spring season at two locations in Hubei Province: Huanggang 30.5°N, 114.6°E) and Xiangyang (Xiangyang, 31.2°N, 112.5°E). The field experiment followed a randomized complete block design with three replicates. Each plot consisted of five rows, each 2.5 m in length, with a planting density of 67,500 plants per hectare. Plants were spaced 0.25 m apart within rows, with 0.5 m spacing between rows. Three seeds were sown per hole, and plots with emergence rates below 98% were excluded from subsequent yield evaluations. At maturity, only the middle three rows of each five-row plot were harvested to evaluate yield-related traits. All ears from the middle three rows were collected, and traits including ear length, ear diameter, kernel number per row, kernel weight per ear, and grain

yield per plot were assessed. The total ear yield from the three rows was recorded, and the number of harvested ears was counted. Grain yield per hectare was calculated using the following:

Grain yield per hectare = Total kernel weight of three rows/Number of ears in three rows x 4500 x 15 (**2**)

Significant differences in traits among hybrids were determined using one-way ANOVA.

Exogenous TPP supplementation

Field-grown *zmtpk2-cr1* mutant plants were treated with exogenous TPP 30 days post-sowing. Three concentrations of TPP solutions (0.02%, 0.04%, and 0.06%; w/v) were administered via foliar spray, with water spray serving as the control. Each treatment was applied five times at 5-day intervals. Ear length was evaluated at the mature stage. For $qKB6.2a^{KUI3}$, $qKB6.2a^{B77}$ and hybrid maize, plants were cultivated in the field and treated with a 0.04% TPP solution 30 days post-sowing. This treatment was applied three times, with a 7-day interval between applications. Phenotypic traits, including plant height, ear height, ear length, ear diameter, ear weight, and plot yield, were measured at maturity. For hybrid rice, field-grown plants were sprayed with a 0.04% TPP solution at the heading stage. The treatment was applied five times at 7-day intervals. Traits measured at maturity, including plant height, grain length, grain width, and thousand-grain weight. And for hybrid rapeseed, plants were grown in the field and sprayed with a 0.04% TPP solution at the bolting stage. The treatment was applied five times at 7-day intervals. Traits assessed at maturity included plant height, silique length, seed size, thousand-seed weight, and seed oil content. The 0.04% TPP solution was applied at 150 L/ha (total of 60 g TPP/ha) via foliar spray. Statistical significance for all traits was determined using one-way ANOVA.

Data availability

RNA-seq data generated in this study have been deposited in the CNGBdb under accession

626 CNP0006828 [https://db.cngb.org/data_resources/project/CNP0006828/]. All biological
627 materials described in this study can be obtained by contacting the corresponding author.
628 Source data are provided with this paper.
629

630 ## References

631 1. Yu, H. & Li, J. Short- and long-term challenges in crop breeding. *Natl Sci Rev* **8**, nwab002
632 (2021).
633 2. Ray, D.K., Mueller, N.D., West, P.C. & Foley, J.A. Yield trends are insufficient to double
634 global crop production by 2050. *PLoS One* **8**, e66428 (2013).
635 3. Jia, H. *et al.* A serine/threonine protein kinase encoding gene *KERNEL NUMBER PER*
636 *ROW6* regulates maize grain yield. *Nat Commun* **11**, 988 (2020).
637 4. Luo, Y. *et al.* Genetic variation in *YIGE1* contributes to ear length and grain yield in maize.
638 *New Phytol* **234**, 513-526 (2022).
639 5. Guan, J.C. *et al.* Divisions of labor in the thiamin biosynthetic pathway among organs of
640 maize. *Front Plant Sci* **5**, 370 (2014).
641 6. Bocobza, S.E. *et al.* Orchestration of thiamin biosynthesis and central metabolism by
642 combined action of the thiamin pyrophosphate riboswitch and the circadian clock in
643 *Arabidopsis*. *Plant Cell* **25**, 288-307 (2013).
644 7. Goyer, A. Thiamine in plants: aspects of its metabolism and functions. *Phytochemistry* **71**,
645 1615-24 (2010).
646 8. Li, X. *et al.* Maize *GOLDEN2-LIKE* genes enhance biomass and grain yields in rice by
647 improving photosynthesis and reducing photoinhibition. *Commun Biol* **3**, 151 (2020).
648 9. Liang, Y., Liu, H.J., Yan, J. & Tian, F. Natural variation in crops: realized understanding,
649 continuing promise. *Annu Rev Plant Biol* (2021).
650 10. Ning, Q. *et al.* An ethylene biosynthesis enzyme controls quantitative variation in maize
651 ear length and kernel yield. *Nat Commun* **12**, 5832 (2021).
652 11. Liu, L. *et al. KRN4* controls quantitative variation in maize kernel row number. *PLoS Genet*
653 **11**, e1005670 (2015).
654 12. Wang, J. *et al. krn1*, a major quantitative trait locus for kernel row number in maize. *New*

655 *Phytol* **223**, 1634-1646 (2019).
656 13. Chen, W. *et al.* Convergent selection of a WD40 protein that enhances grain yield in maize
657 and rice. *Science* **375**, eabg7985 (2022).
658 14. Yang, N. *et al.* Genome assembly of a tropical maize inbred line provides insights into
659 structural variation and crop improvement. *Nat Genet* **51**, 1052-1059 (2019).
660 15. Sun, Q. *et al.* A *NAC-EXPANSIN* module enhances maize kernel size by controlling
661 nucellus elimination. *Nat Commun* **13**, 5708 (2022).
662 16. Li, Y.X. *et al.* Cis-regulatory variation affecting gene expression contributes to the
663 improvement of maize kernel size. *Plant J* **111**, 1595-1608 (2022).
664 17. Jin, M. *et al. ZmCOL3*, a CCT gene represses flowering in maize by interfering with the
665 circadian clock and activating expression of *ZmCCT*. *J Integr Plant Biol* **60**, 465-480
666 (2018).
667 18. Su, H. *et al.* Identification of *ZmNF-YC2* and its regulatory network for maize flowering
668 time. *J Exp Bot* **72**, 7792-7807 (2021).
669 19. Liu, S. *et al.* Mapping regulatory variants controlling gene expression in drought response
670 and tolerance in maize. *Genome Biol* **21**, 163 (2020).
671 20. Wang, X. *et al.* Genetic variation in *ZmVPP1* contributes to drought tolerance in maize
672 seedlings. *Nat Genet* **48**, 1233-41 (2016).
673 21. Sun, X. *et al.* The role of transposon inverted repeats in balancing drought tolerance and
674 yield-related traits in maize. *Nat Biotechnol* **41**, 120-127 (2023).
675 22. Jiang, H. *et al.* Natural polymorphism of *ZmICE1* contributes to amino acid metabolism
676 that impacts cold tolerance in maize. *Nat Plants* **8**, 1176-1190 (2022).
677 23. Sun, G. *et al.* A role for heritable transcriptomic variation in maize adaptation to temperate
678 environments. *Genome Biol* **24**, 55 (2023).
679 24. Rodriguez-Leal, D., Lemmon, Z.H., Man, J., Bartlett, M.E. & Lippman, Z.B. Engineering
680 quantitative trait variation for crop improvement by genome editing. *Cell* **171**, 470-480.e8
681 (2017).
682 25. Chen, K., Wang, Y., Zhang, R., Zhang, H. & Gao, C. CRISPR/Cas genome editing and
683 precision plant breeding in agriculture. *Annu Rev Plant Biol* **70**, 667-697 (2019).
684 26. Liu, L. *et al.* Enhancing grain-yield-related traits by CRISPR-Cas9 promoter editing of

685 maize *CLE* genes. *Nat Plants* **7**, 287-294 (2021).
686 27. Wang, Y., Tang, Q., Pu, L., Zhang, H. & Li, X. CRISPR-Cas technology opens a new era
687 for the creation of novel maize germplasms. *Frontiers in Plant Science* **13**(2022).
688 28. Li, S. *et al.* Improving yield-related traits by editing the promoter of the heading date gene
689 Ehd1 in rice. *Theor Appl Genet* **136**, 239 (2023).
690 29. Xiao, Y. *et al.* Genome-wide dissection of the maize ear genetic architecture using multiple
691 populations. *New Phytol* **210**, 1095-1106 (2016).
692 30. Pan, Q. *et al.* Genome-wide recombination dynamics are associated with phenotypic
693 variation in maize. *New Phytol* **210**, 1083-94 (2016).
694 31. Peng, Y. *et al.* Chromatin interaction maps reveal genetic regulation for quantitative traits
695 in maize. *Nat Commun* **10**, 2632 (2019).
696 32. Marand, A.P. et al. The genetic architecture of cell type-specific cis regulation in maize.
697 Science 388, eads6601 (2025).
698 33. Chen, L. *et al.* Genome sequencing reveals evidence of adaptive variation in the genus *Zea*.
699 *Nat Genet* **54**, 1736-1745 (2022).
700 34. Ertiro, B.T. *et al.* Comparison of Kompetitive Allele Specific PCR (KASP) and genotyping
701 by sequencing (GBS) for quality control analysis in maize. *BMC Genomics* **16**, 908 (2015).
702 35. Frank, R.A., Leeper, F.J. & Luisi, B.F. Structure, mechanism and catalytic duality of
703 thiamine-dependent enzymes. *Cell Mol Life Sci* **64**, 892-905 (2007).
704 36. Li, J., Kim, Y.J. & Zhang, D. Source-to-sink transport of sugar and its role in male
705 reproductive development. *Genes (Basel)* **13** (2022).
706 37. Li, M., Zhong, W., Yang, F. & Zhang, Z. Genetic and molecular mechanisms of quantitative
707 trait loci controlling maize inflorescence architecture. *Plant Cell Physiol* **59**, 448-457
708 (2018).
709 38. Gerdes, S. *et al.* Plant B vitamin pathways and their compartmentation: a guide for the
710 perplexed. *J Exp Bot* **63**, 5379-95 (2012).
711 39. Woodward, J.B. *et al.* A maize thiamine auxotroph is defective in shoot meristem
712 maintenance. *Plant Cell* **22**, 3305-17 (2010).
713 40. Wang, Y. *et al.* A spatial transcriptome map of the developing maize ear. *Nat Plants* **10**,
714 815-827 (2024).

41. Sun, Y. *et al.* Progressive meristem and single-cell transcriptomes reveal the regulatory mechanisms underlying maize inflorescence development and sex differentiation. *Mol Plant* **17**, 1019-1037 (2024).
42. Didangelos, T. *et al.* Efficacy and safety of the combination of palmitoylethanolamide, superoxide dismutase, alpha lipoic acid, vitamins B12, B1, B6, E, Mg, Zn and nicotinamide for 6 months in people with diabetic neuropathy. *Nutrients* **16**, (2024).
43. Nozaki, S. *et al.* Thiamine tetrahydrofurfuryl disulfide improves energy metabolism and physical performance during physical-fatigue loading in rats. *Nutr Res* **29**, 867-72 (2009).
44. Frelin, O. *et al.* Identification of mitochondrial thiamin diphosphate carriers from *Arabidopsis* and maize. *Funct Integr Genomics* **12**, 317-26 (2012).
45. Abramson, J. *et al.* Accurate structure prediction of biomolecular interactions with AlphaFold 3. *Nature* **630**, 493-500 (2024).
46. Liu, H. *et al.* CRISPR-P 2.0: CRISPR-P 2.0: An improved CRISPR-Cas9 tool for genome editing in Plants. *Mol Plant* **10**, 530-532 (2017).
47. Li, C. *et al.* RNA-guided Cas9 as an *in vivo* desired-target mutator in maize. *Plant Biotechnol J* **15**, 1566-1576 (2017).
48. Liu, H.J. *et al.* High-throughput CRISPR/Cas9 mutagenesis streamlines trait gene identification in maize. *Plant Cell* **32**, 1397-1413 (2020).
49. Rao, X., Huang, X., Zhou, Z. & Lin, X. An improvement of the 2^(-delta delta CT) method for quantitative real-time polymerase chain reaction data analysis. *Biostat Bioinforma Biomath* **3**, 71-85 (2013).
50. Bolger, A.M., Lohse, M. & Usadel, B. Trimmomatic: a flexible trimmer for Illumina sequence data. *Bioinformatics* **30**, 2114-20 (2014).
51. Lowe, K. *et al.* Rapid genotype "independent" *Zea mays* L. (maize) transformation via direct somatic embryogenesis. *In Vitro Cell Dev Biol Plant* **54**, 240-252 (2018).
52. Yoo, S.D., Cho, Y.H. & Sheen, J. *Arabidopsis* mesophyll protoplasts: a versatile cell system for transient gene expression analysis. *Nat Protoc* **2**, 1565-72 (2007).
53. Huang, M. *et al.* Camouflage patterning in maize leaves results from a defect in porphobilinogen deaminase. *Mol Plant* **2**, 773-789 (2009).
54. Lee, B.L., Ong, H.Y. & Ong, C.N. Determination of thiamine and its phosphate esters by

gradient-elution high-performance liquid chromatography. *J Chromatogr* **567**, 71-80 (1991).

55. Zheng, H., Zhang, Q., Quan, J., Zheng, Q. & Xi, W. Determination of sugars, organic acids, aroma components, and carotenoids in grapefruit pulps. *Food Chem* **205**, 112-21 (2016).
56. Chen, W. *et al.* A novel integrated method for large-scale detection, identification, and quantification of widely targeted metabolites: application in the study of rice metabolomics. *Mol Plant* **6**, 1769-80 (2013).
57. Salem, M.A., Jüppner, J., Bajdzienko, K. & Giavalisco, P. Protocol: a fast, comprehensive and reproducible one-step extraction method for the rapid preparation of polar and semi-polar metabolites, lipids, proteins, starch and cell wall polymers from a single sample. *Plant Methods* **12**, 45 (2016).
58. Yan, S., Huang, W., Gao, J., Fu, H. & Liu, J. Comparative metabolomic analysis of seed metabolites associated with seed storability in rice (*Oryza sativa* L.) during natural aging. *Plant Physiol Biochem* **127**, 590-598 (2018).
59. Ajjawi, I., Rodriguez Milla, M.A., Cushman, J. & Shintani, D.K. Thiamin pyrophosphokinase is required for thiamin cofactor activation in *Arabidopsis*. *Plant Mol Biol* **65**, 151-62 (2007).
60. Rapala-Kozik, M., Gołda, A. & Kujda, M. Enzymes that control the thiamine diphosphate pool in plant tissues. Properties of thiamine pyrophosphokinase and thiamine-(di)phosphate phosphatase purified from *Zea mays* seedlings. *Plant Physiol Biochem* **47**, 237-42 (2009).

Acknowledgements

This research was supported by funding from the National Natural Science Foundation of China (32321005, 32301840), the China Postdoctoral Science Foundation (2023M731239), Natural Science Foundation of Hubei Province, China (2023AFB261) and the 111 Project Crop Genomics and Molecular Breeding (B20051). Computation resources were provided by the high-throughput computing platform of the National Key Laboratory of Crop Genetic Improvement at Huazhong Agricultural University and supported by H.Liu. We sincerely thank Qun Zhang from Huanggang Academy of Agricultural Sciences for his assistance with rice

cultivation, TPP application, and field plot yield measurements. We also extend our gratitude to Dr. Yixian Song and Dr. Yushun Jiao from Huazhong Agricultural University for their valuable support in rapeseed cultivation and phenotypic evaluation of yield-related traits. Thanks to Dr. Shijuan Yan from the Guangdong Academy of Agricultural Sciences for providing the metabolomics platform and conducting the metabolomic analysis of maize kernel.

Author contributions

J.B.Y., Y. Luo, and Y. Liu conceived and designed the study. Y. Luo, Y. Liu, and H.N.L. performed fine mapping, transgenic validation, and *ZmTPK2* breeding value assessment. Y. Luo and X.J.L. carried out protein expression and enzymatic activity assays. Y. Luo, Y. W., and J.L.Z. conducted the evaluation of the breeding value of exogenous TPP applications in maize, rice, and rapeseed hybrids. Y.B.W. and W.J.F. performed the RNA-seq analysis. W.Q.L. managed field planting and material collection. Y. Luo wrote the manuscript. J.B.Y., J.L., A.R. Fernie, L.M.J., L.Zh., and J.P.Zh. revised the manuscript. All authors discussed the results, contributed to data interpretation, and approved the final manuscript.

Competing interests

Y. Luo, Y. Liu, H.N.L, and J.B.Y are co-inventors on two patents related to the findings reported in this study. The first patent (filing number: 2024113919997) covers the development and application of molecular markers for the maize ear length and yield gene *ZmTPK2*. The second patent (filing number: 2024113559050) concerns increasing maize ear length and yield through overexpression of *ZmTPK2* and exogenous application of TPP. All other authors declare no competing interests.

Figures legends

Fig. 1. Positional cloning and functional validation of *qKB6.2a*. a, b Phenotypic comparison of ears (**a**) and female inflorescence meristem (**b**) between the NILs. **c-f** Comparison of inflorescence meristem length (**c**), floret number per row (**d**), kernel number per row (**e**) and ear length (**f**) between $qKB6.2a^{KUI3}$ and $qKB6.2a^{B77}$. **g** Fine mapping narrowed *qKB6.2a* to a

~58.2 kb interval containing two candidate genes, *Zm00001d037915* and *Zm00001d037916*. **h, i** Expression levels of *Zm00001d037915* (**h**) and *Zm00001d037916* (**i**) in the 2-5 mm developing female ears of NILs. Gene-expression level was measured by RT-qPCR using three biological replicates and three technical replicates per sample, normalized to maize *Actin* gene (*Zm00001d010159*). **j** Gene structure and polymorphisms of *ZmTPK2* between NILs. Two SNPs in the promoter, one SNP and an insertion in CRE ~41.8 kb upstream of *ZmTPK2* were identified. **k** Transient expression assays assessing the effects of *ZmTPK2* promoter and CRE variants on relative LUC/REN activity. Constructs and results are shown schematically on the left and in boxplots on the right. $pZmTPK2^{KUI3}$ and $pZmTPK2^{B77}$, the promoter of *ZmTPK2* from $qKB6.2a^{KUI3}$ and $qKB6.2a^{B77}$, respectively; $p*ZmTPK2^{KUI3\ C\text{-}T}$, the point mutation at SNP C to T in $pZmTPK2^{KUI3}$; $p*ZmTPK2^{KUI3\ A\text{-}G}$, the point mutation at SNP A to G in $pZmTPK2^{KUI3}$; $cre{+}pZmTPK2^{KUI3}$ and $cre{+}pZmTPK2^{B77}$, the CRE and promoter of *ZmTPK2* from $qKB6.2a^{KUI3}$ and $qKB6.2a^{B77}$, respectively; $cre*{+}pZmTPK2^{B7\ +AAAAT}$, the insertion of AAAAT in $creZmTPK2^{B77}$; $cre*{+}pZmTPK2^{B77\ T\text{-}C}$, the point mutation at SNP T to C in $creZmTPK2^{B77}$. LUC, Firefly luciferase; REN, Renilla luciferase; Ter, nopaline synthase terminator. Transient expression in maize leaf protoplasts was conducted with four to six biological replicates per construct. Data represent mean ± SD. **l, m** Major haplotypes identified in a diverse association mapping panel (**l**) and haplotype frequency of *ZmTPK2* (**m**), based on promoter and CRE variations. Data Statistical significance was determined by a one-way ANOVA analysis in (**c-f, h, i**), and Tukey's multiple comparisons in ($P \leq 0.05$, **k**). Scale bar = 2 cm in (**a**) and 100 μm in (**b**). Source data are provided as a Source Data file.

Fig. 2. *ZmTPK2* finely regulates ear length and ear weight. **a, b** *ZmTPK2* knockout mutants (*tpk2-cr1* and *tpk2-cr2*) produce shorter plant and ears compared to their non-transgenic (NT) siblings in Jilin, China. **c-e** Comparison of ear traits between NT and *tpk2-cr* plants, including ear length (**c**), kernel number per row (**d**), and ear weight (**e**). **f, g** Plant (**f**) and ear status (**g**) of NT and *ZmTPK2* overexpression (*TPK2-OE1~OE7*) lines. **h-j** Comparison of relative *ZmTPK2* expression levels in developing ear (**h**), ear length (**i**) and kernel weight per ear (**j**) between NT and *TPK2-OE1~OE7* lines. Violin plots show the distribution of the data, with the central line indicating the median. Dots represent biologically independent plants, and sample sizes (n) are

indicated below each group. **k**, **l** Comparison of *ZmTPK2* expression in developing ear (**k**), and ear length (**l**) among *Hap1*, *Hap2*, *Hap3* and *Hap4* maize inbred lines. Due to the limited sample size of *Hap1*, statistical analysis was conducted only on *Hap2*, *Hap3* and *Hap4*. Data are shown as mean ± SD, and error bars denote standard deviation among biological replicates. **m** A conceptual representation of the observed correlation between *ZmTPK2* expression levels and ear length across natural haplotypes and overexpression lines. Gene-expression level was quantified by RT-qPCR with three biological replicates and three technical replicates per sample, normalized to the maize *Actin* gene (*Zm00001d010159*) in (**h, k**). All expression levels were standardized to NT control. Statistical significance was determined by a one-way ANOVA analysis in (**c-e**), and multiple comparisons (Tukey's test) in (**h-l**) with significant differences indicated by different letters ($P < 0.05$). Scale bar = 20 cm in (**a, f**) and 2 cm in (**b, g**). Source data are provided as a Source Data file.

Fig. 3. *ZmTPK2* indirectly regulates kernel yield and quality by modulating energy metabolism and photosynthetic activity. a Thiamine pyrophosphokinase (TPK) converts thiamine to thiamine pyrophosphate (TPP) in plants. **b** Enzymatic activity of ZmTPK2 compared to negative control at varying thiamine concentrations, modeled by Michaelis-Menten kinetics. Data represent mean ± SD from three biologically independent replicates. **c-e** Endogenous TPP levels measured in leaves and 2-5 mm ears of *tpk2-cr1* mutants (**c**), and *TPK2-OE* lines (**d, e**). **f, g** Phenotypic rescue of *tpk2-cr1* ear length phenotype by exogenous TPP supplementation. Representative ear images (**f**) and mean ear length (**g**) of *tpk2-cr1* mutants following 0.02%, 0.04% and 0.06% TPP treatments via foliar spray. **h-k** Net photosynthetic (**h, j**) and respiratory rates (**i, k**) of *tpk2-cr1* and overexpression plants versus controls. **l-q** Metabolomic analysis, starch, and protein analysis on mature kernels of *tpk2-cr1* (**l-n**) and *TPK2-OE2* and *TPK2-OE7* overexpression lines (**o-q**). **r** Proposed model of *ZmTPK2* fine-tuning TPP levels to regulate energy metabolism, grain yield, and protein content. Black dots indicate individual samples. Bars represent mean ± SD, and error bars show variability among biological replicates. Statistical significance was assessed using one-way ANOVA for (**c**, **h**, **i, l-n**) and multiple comparison tests (Tukey's test) for (**d, e, g, j, k, o-q**), with distinct letters indicating significant differences ($P < 0.05$). Scale bar in (**f**) represents 2 cm. Source

data are provided as a Source Data file.

Fig. 4. Natural favorable haplotype of *ZmTPK2* boosts yield-related traits in hybrids. a, b Plant architecture (**a**) and ears morphology (**b**) of hybrids, generated from direct crossing of $qKB6.2a^{KUI3}$ and $qKB6.2a^{B77}$ with four elite maize inbred lines (PH4CV, Jing92, Zheng58 and V76-1). **c-f** Evaluation of yield-associated traits, including ear length (**c**), grain yield (**d**), kernel number per row (**e**), and ear diameter (**f**). **g** Relative *ZmTPK2* expression levels in mature leaves of these eight hybrids. Violin plots show the data distribution density. Dashed lines indicate the median (central) and the interquartile range (upper and lower). Each dot represents the phenotype value of an independent biological sample; blue dots indicate F_1 hybrids derived from a line carrying $qKB6.2a^{KUI3}$ × inbred line, and purple dots indicate F_1 hybrids derived from a line $qKB6.2a^{B77}$ × inbred line. The level of significance is determined by a one-way ANOVA analysis. Scale bar = 20 cm in (**a**) and 2 cm in (**b**). Source data are provided as a Source Data file.

Fig. 5 Treatment with 0.04% thiamine pyrophosphate (TPP) solution significantly enhances yield in maize, rice and rapeseed. a Plant architecture and ear morphology of maize hybrids under water (control) and 0.04% (w/v) TPP solution treatment. **b**, **c** Comparison of ear length (**b**) and grain yield (**c**) of maize hybrids under 0.04% TPP treatment vs. control. **d** Plant architecture and kernel appearance of rice hybrids under TPP treatment and control. **e** Comparison of grain yield under treatment with water and 0.04% TPP solution treatments. **f** Plant architecture, silique morphology, and seed characteristics of rapeseed hybrids under both conditions. **g-j** Quantitative comparisons of silique length (**g**), seed size (**h**), thousand seed weight (**i**), and seed oil content (**j**) under control and 0.04% TPP solution treatment. Violin plots display data distribution, with dashed lines marking the median and interquartile range. Each dot corresponds to an independent biological replicate (blue, control; orange, 0.04% TPP treatment). The level of significance is determined by a one-way ANOVA analysis. Scale bar: 20 cm for maize plants, 2 cm for maize ears (**a**); 10 cm for rice plants, 1cm for rice kernels (**d**); 10 cm for rapeseed plants, 1 cm for siliques, and 2mm for seeds (**f**). Source data are provided as a Source Data file.

Editor's Summary

Thiamine pyrophosphate (TPP) is the biologically active form of vitamin B1 and servers as an essential metabolic cofactor regulating energy production, redox homeostasis, and carbon assimilation. Here, the authors show that optimizing TPP metabolism can enhance yield and quality in maize, rice and rapeseed.

Peer review information: *Nature Communications* thanks James Schnable and the other, anonymous, reviewer(s) for their contribution to the peer review of this work. A peer review file is available.

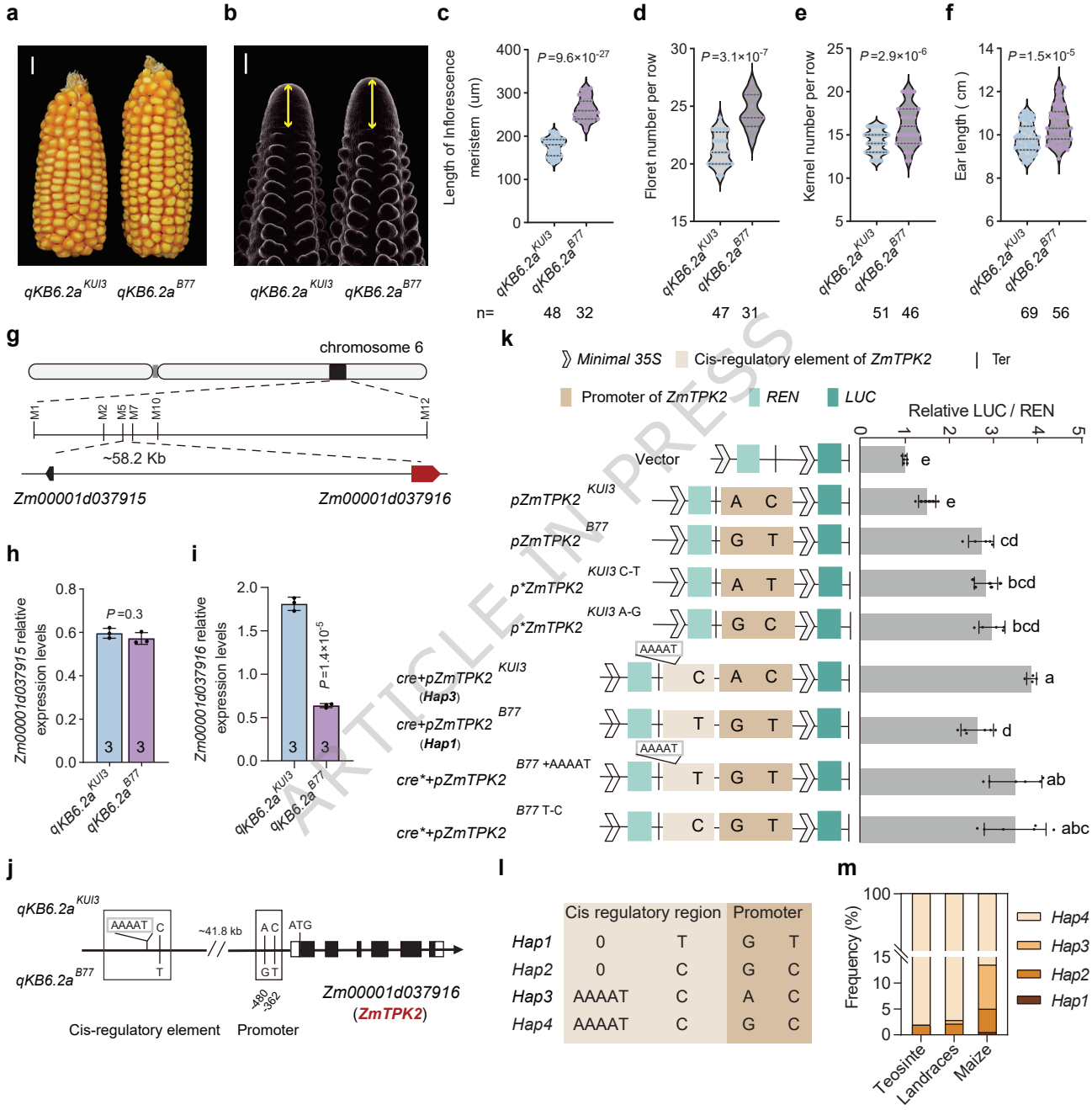

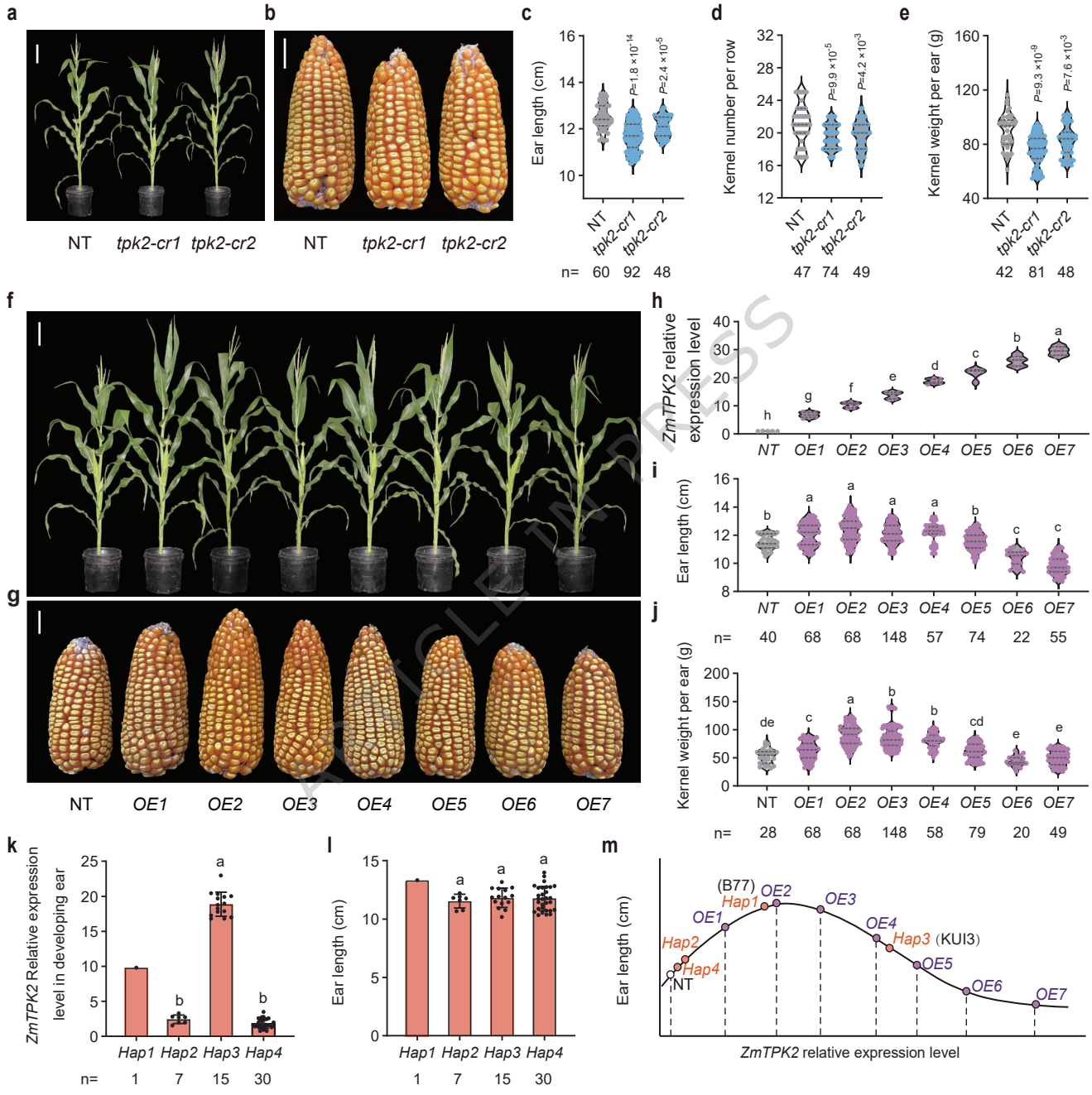
a
b
NT
tpk2-cr1
tpk2-cr2
c
Ear length (cm)
P=1.8 ×10-14
P=2.4 ×10-5
n= 60 92 48
d
Kernel number per row
P=9.9 ×10-5
P=4.2 ×10-3
47 74 49
e
Kernel weight per ear (g)
P=9.3 ×10-9
P=7.6 ×10-3
42 81 48
f
g
NT
OE1
OE2
OE3
OE4
OE5
OE6
OE7
h
ZmTPK2 relative expression level
i
Ear length (cm)
j
Kernel weight per ear (g)
n= 40 68 68 148 57 74 22 55
n= 28 68 68 148 58 79 20 49
k
ZmTPK2 Relative expression level in developing ear
Hap1
Hap2
Hap3
Hap4
n= 1 7 15 30
l
Ear length (cm)
1 7 15 30
m
Ear length (cm)
(B77)
Hap1
OE2
OE3
OE1
OE4
Hap2
Hap3 (KUI3)
Hap4
NT
OE5
OE6
OE7
ZmTPK2 relative expression level

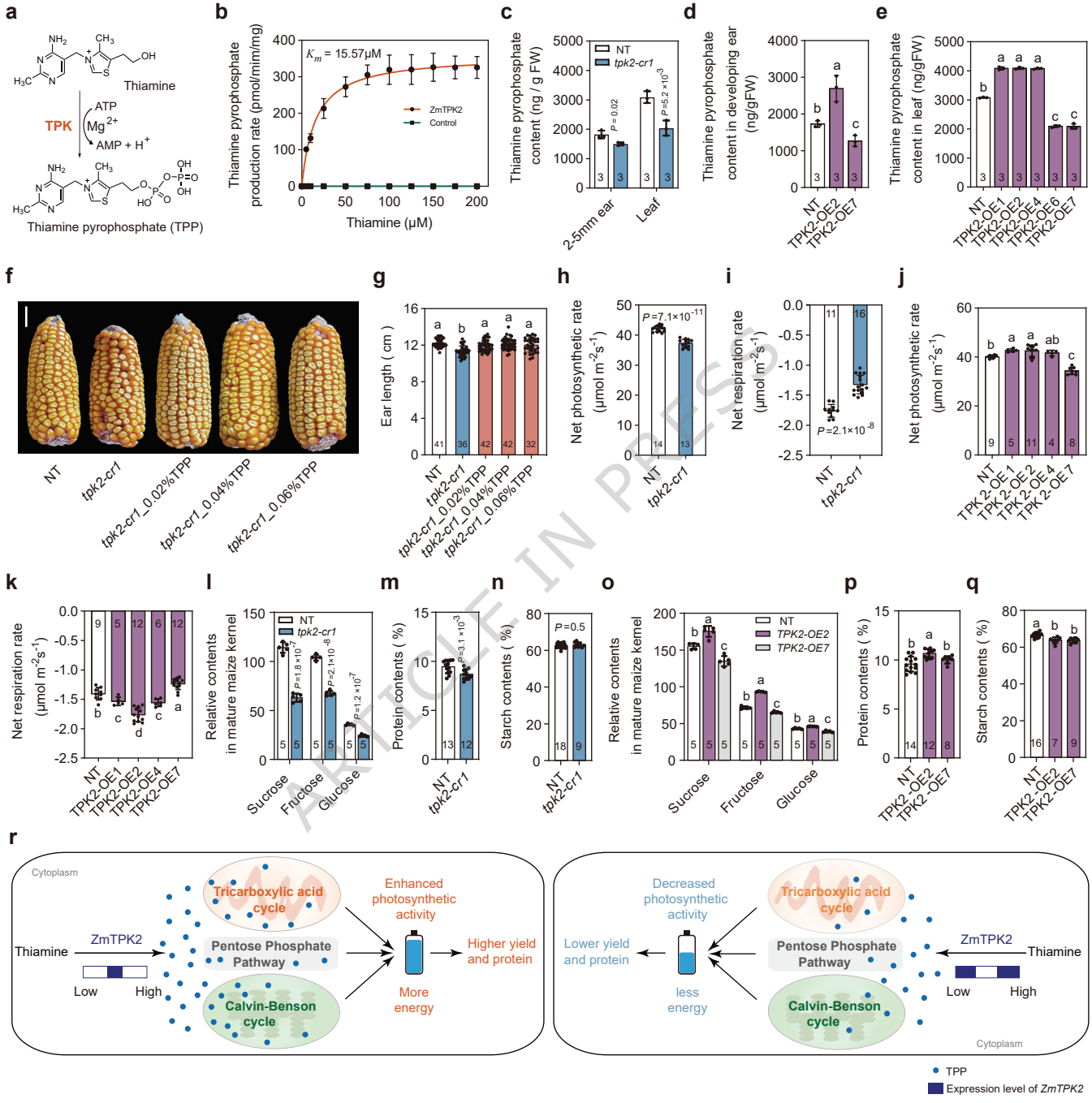

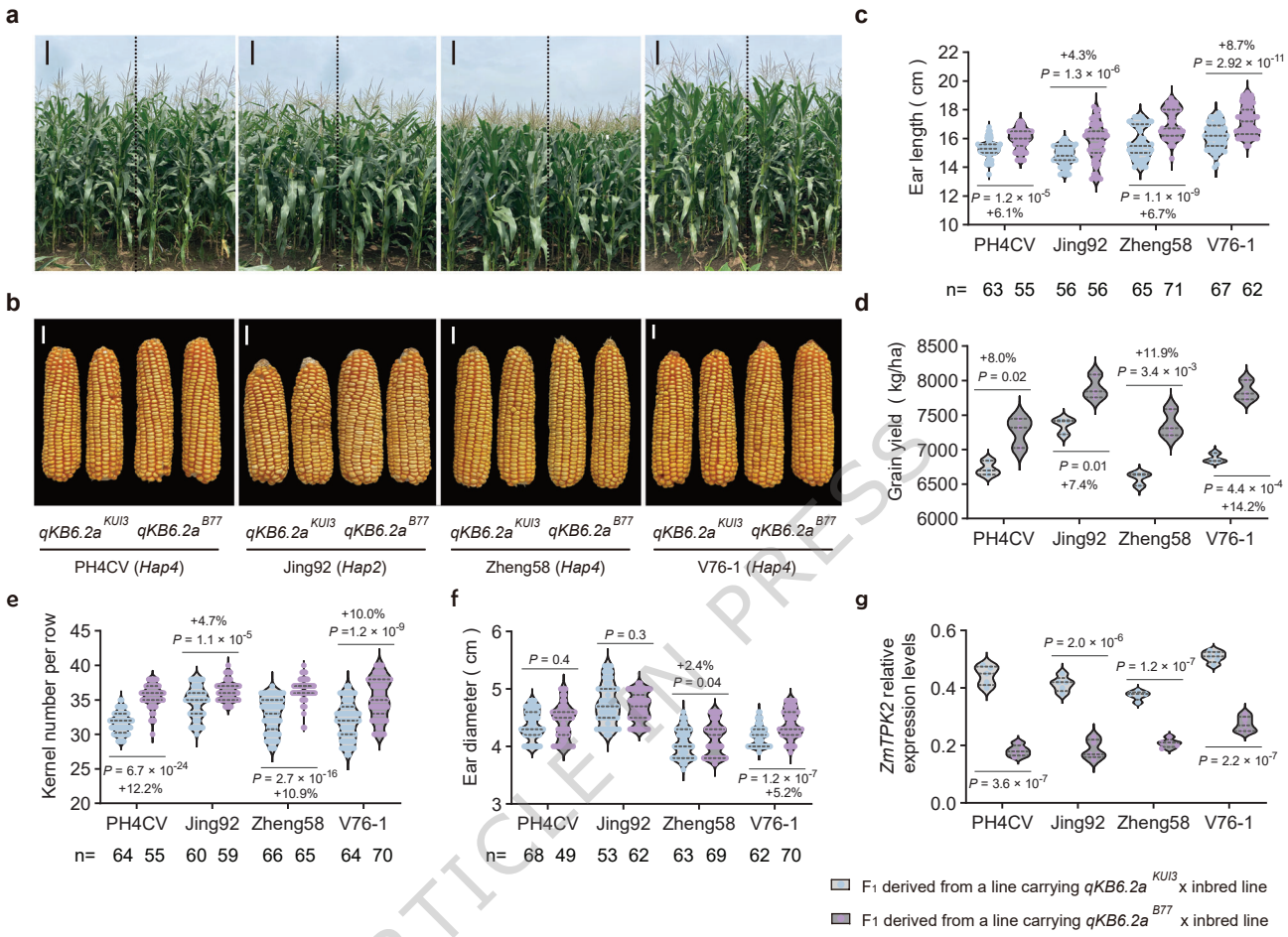

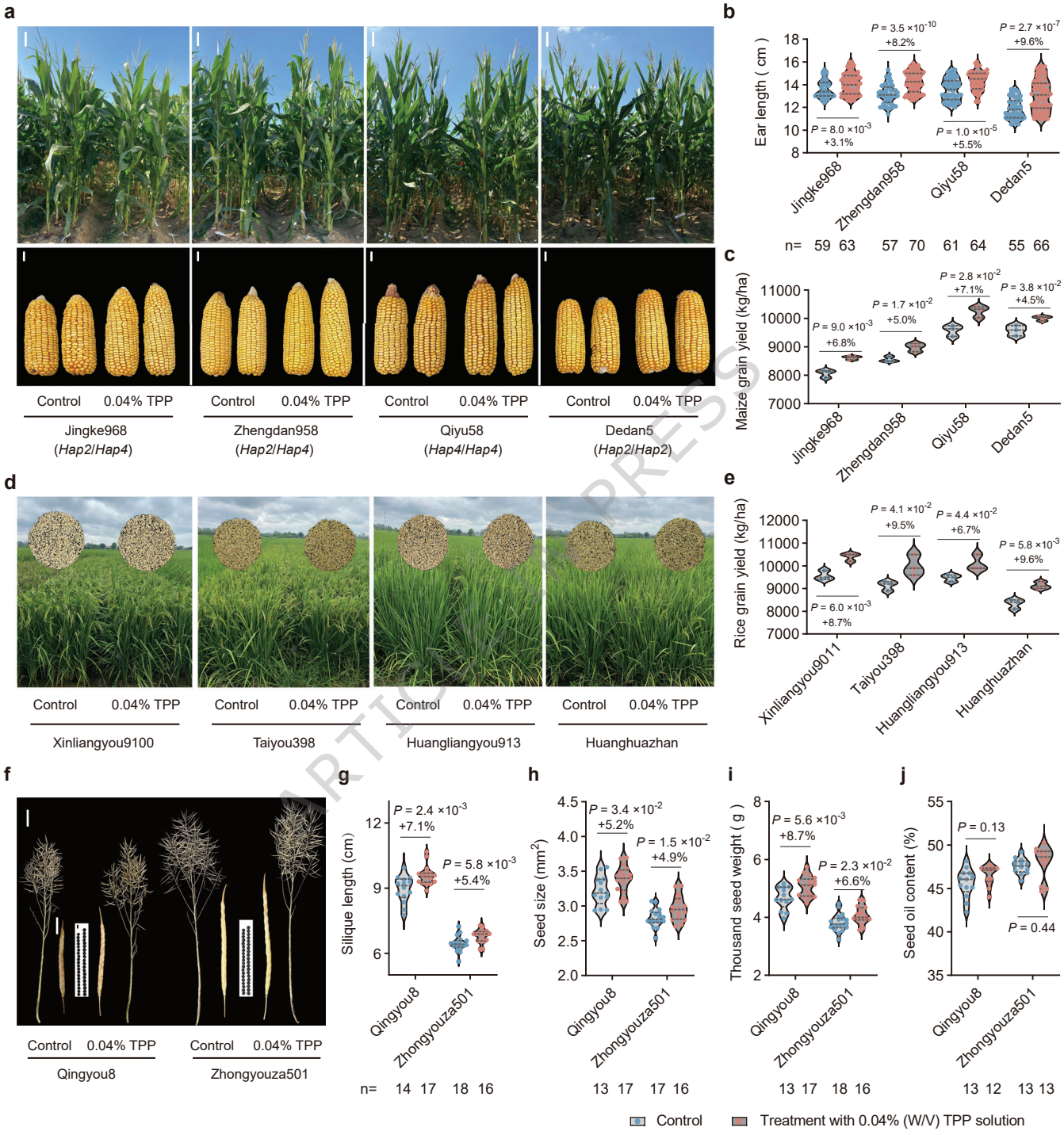
a
Control
0.04% TPP
Jingke968
(Hap2/Hap4)
Zhengdan958
(Hap2/Hap4)
Qiyu58
(Hap4/Hap4)
Dedan5
(Hap2/Hap2)
b
Ear length (cm)
P = 8.0 ×10-3
+3.1%
P = 3.5 ×10-10
+8.2%
P = 1.0 ×10-5
+5.5%
P = 2.7 ×10-7
+9.6%
n= 59 63 57 70 61 64 55 66
c
Maize grain yield (kg/ha)
P = 9.0 ×10-3
+6.8%
P = 1.7 ×10-2
+5.0%
P = 2.8 ×10-2
+7.1%
P = 3.8 ×10-2
+4.5%
d
Xinliangyou9100
Taiyou398
Huangliangyou913
Huanghuazhan
e
Rice grain yield (kg/ha)
P = 6.0 ×10-3
+8.7%
P = 4.1 ×10-2
+9.5%
P = 4.4 ×10-2
+6.7%
P = 5.8 ×10-3
+9.6%
f
Qingyou8
Zhongyouza501
g
Silique length (cm)
P = 2.4 ×10-3
+7.1%
P = 5.8 ×10-3
+5.4%
n= 14 17 18 16
h
Seed size (mm2)
P = 3.4 ×10-2
+5.2%
P = 1.5 ×10-2
+4.9%
13 17 17 16
i
Thousand seed weight (g)
P = 5.6 ×10-3
+8.7%
P = 2.3 ×10-2
+6.6%
13 17 18 16
j
Seed oil content (%)
P = 0.13
P = 0.44
13 12 13 13
Control
Treatment with 0.04% (W/V) TPP solution